ChemComm

COMMUNICATION

View Article Online
View Journal

Cite this: DOI: 10.1039/d0cc01850c

Received 10th March 2020,
Accepted 11th May 2020

DOI: 10.1039/d0cc01850c

rsc.li/chemcomm

Cellulose nanocrystals of variable sulfation degrees can sequester specific platelet lysate-derived biomolecules to modulate stem cell response†

Bárbara B. Mendes, [ab] Manuel Gómez-Florit, [ab] Hugo Osório, [c] Adriana Vilaça, [ab] Rui M. A. Domingues, *[ab] Rui L. Reis [ab] and Manuela E. Gomes *[ab]

The surface chemistry of cellulose nanocrystals was engineered to show variable sulfation degrees, which was exploited to modulate platelet lysate-derived biomolecule sequestration and presentation. The protein coronas developed on CNC surfaces were characterized and it was demonstrated how they promote different signaling effects on human adipose-derived stem cell behavior.

Cellulose nanocrystals (CNCs) have been increasingly used for multiple tissue engineering (TE) applications due to their outstanding mechanical properties, easy surface functionalization, complex rheological behavior and minimal toxicity.[1] We have recently developed injectable platelet lysate (PL) based hydrogels reinforced with CNCs.[2] In this nanocomposite biomaterial, an inexpensive human-based source of supra-physiological doses of multiple signaling molecules known to modulate different cell functions, including adhesion, proliferation and differentiation, was used.[3] It was demonstrated that the increase of CNC content had a positive impact on the biomaterial cell supportive potential due to the improvement of the physical properties. It was also suggested that these positive effects may be correlated with the possible sequestration and solid phase presentation of PL signaling proteins anchored onto the CNC surfaces, emulating a biomimetic mechanism, which has been increasingly recognized to increase the half-life and boost the bioactivity of signaling molecules such as growth factors (GFs). However, the nature and extent of these CNC–PL protein interactions and how they can be leveraged to guide cell fate have not been demonstrated.

[a] *3B's Research Group, I3Bs – Research Institute on Biomaterials, Biodegradables and Biomimetics, University of Minho, Headquarters of the European Institute of Excellence on Tissue Engineering and Regenerative Medicine, Avepark, Parque de Ciência e Tecnologia, Zona Industrial da Gandra, Barco, Guimarães, Portugal. E-mail: megomes@i3bs.uminho.pt, rui.domingues@i3bs.uminho.pt*

[b] *ICVS/3B's – PT Government Associate Laboratory, Braga/Guimarães, Portugal*

[c] *Instituto de Investigação e Inovação em Saúde (I3S), Universidade do Porto, Porto, Portugal*

† Electronic supplementary information (ESI) available: Experimental materials and methods. See DOI: 10.1039/d0cc01850c

It is well known that upon introduction into complex biological fluid (*e.g.*, human blood plasma contains more than 3700 proteins), nanomaterials are rapidly covered by a layer of proteins known as a protein corona.[4] Conceptually, an initial corona is typically formed from the highly abundant proteins, consisting of a more loosely associated and rapidly exchanging layer of biomolecules (called the 'soft' corona).[4,5] These biomacromolecules undergo rapid exchange with the biological environment, being displaced over time from the nanomaterial surface by proteins with a higher binding affinity and a slower exchange rate (called the 'hard' corona).[4,5] In an *in vivo* scenario, nanomaterials interact with thousands of different types of proteins that define their lifetime, physicochemical properties (*e.g.*, protein conformation, hydrodynamic size and surface charge), and subsequently their biological identity (*e.g.*, cytotoxicity, biodistribution, and endocytosis into specific cells).[6]

The surface chemistry of nanomaterials is among the most significant factors determining the amount and composition of the hard corona.[6] Tuning the protein corona by tailoring the chemical composition of nanoparticles has been widely explored in nanomedicine to adjust their functionality as, *e.g.*, drug carriers or abiotic protein affinity reagents.[7] Remarkably, it has been demonstrated that the more abundantly associated proteins are not necessarily responsible for the most significant effect at the cell–nanomaterial interfaces, since a less abundant protein with high specificity for a particular receptor could trigger a crucial biological process.[4b,6] Therefore, our hypothesis is that by modulating the surface chemistry of CNCs to recruit specific signaling biomolecules from PL to the nanoparticle surface, it would be possible to tune the composition of their protein corona. In the development of PL–CNC biomaterials, this strategy would provide a new tool to define the biological identity of cell microenvironment and thus control their fate in TE strategies based on this xeno-free cell matrix.

The most typical production method of CNCs, which was also adopted in this study, is based on the hydrolysis of sulfuric acid.[8] During this process, CNCs are simultaneously grafted

with anionic sulfate ester groups on their surface, which are responsible for their colloidal stability in aqueous solutions. Interestingly, in mammalian tissues, protein binding by membrane or extracellular matrix sulfated glycosaminoglycans (GAGs), such as heparin and heparan sulfate, is known to play key roles in potentiating protein cell signaling and in protecting them from proteolytic degradation.[9] This GAG mediated presentation and stabilization of a wide range of proteins (*e.g.*, GFs, adhesion proteins, and chemokines) is dominated by electrostatic interactions but also includes contributions from hydrogen bonding, van der Waals interaction, and hydrophobic interactions.[10] Numerous functional GAG mimetic biomaterials have been developed, including supramolecular nanostructures displaying different sulfated monosaccharide motifs on their surfaces, which could regulate the bioactivity of GFs *in vitro* and *in vivo* in a sulfation pattern dependent manner.[11] Inspired by these functional nanostructures acting as GAG analogs, in this work, we produced CNCs with variable sulfation degrees in their surface glucose units (Fig. 1). First, CNCs were produced from microcrystalline cellulose resulting in typical rod-shaped and negatively charged nanoparticles (Fig. 1).[8] Afterwards, this CNC suspension with a high sulfation degree (H-CNC) was hydrothermally treated in an autoclave.[12] At high temperatures, an *in situ* acid autocatalyzed desulfation reaction occurs, promoting the hydrolysis of sulfate half-ester groups and their conversion to hydroxyl groups.[12] We hydrothermally treated the original H-CNC (292 ± 5 mmol kg^{-1}) suspension for 3 or 6 hours at 120 °C to obtain CNCs with medium (M-CNC, 233 ± 4 mmol kg^{-1}) and low (L-CNC, 88.6 ± 0.4 mmol kg^{-1}) sulfation degrees, respectively (Fig. S1A and B, ESI†), as confirmed by conductometric titration measurements (Fig. S2B, ESI†). To maintain the possibility of reacting with PL proteins through reversible Schiff base bonds and following the concept that we have previously proposed for PL–CNC hydrogels,[2] three CNC formulations with different sulfation degrees were then aldehyde-modified (a-CNC) by sodium periodate oxidation and their surface charge was analyzed by zeta potential measurements (Fig. S1C, ESI†). The CNC morphology exhibited a non-significant variability of nanoparticle dimensions, and thus of surface area, between formulations (Fig. S2A, ESI†).

Previous studies on GAG mimetic polymers have shown that they can establish favorable interactions with GFs and thus boost their bioactivities, namely, increase cell proliferation (induced by fibroblast growth factor-2) or osteogenic differentiation potential (induced by bone morphogenic protein-2).[13] In contrast to cellulose sulfate derivatives that are relatively flexible and have excellent water solubility, CNCs are stiff solid particles that exhibit an amphiphilic character. This character stems from the cellulose chain packing that, besides the hydroxyl and sulfate hydrophilic groups, also results in a hydrophobic crystalline plane due to which axial CH moieties are exposed at the surface of the nanocrystals.[14] These physical and chemical properties of CNCs, much different from those of soluble cellulose sulfate derivatives, will certainly contribute to the entity of the protein corona built on the material surface, as well as their release kinetics and further presentation in the cellular microenvironment.[4b]

CNCs with different sulfation degrees were incubated with PL solution to investigate the impact on the composition of the protein corona (Fig. 2 and Fig. S3, ESI†). First, we studied the protein composition of the 'soft' and 'hard' corona according their molecular weight by SDS-PAGE (Fig. S3A, ESI†). Increasing the surface charge density led to an increase in protein adsorption and in PL–CNC complex pellet size, as reflected by the intensity of the bands present in the gel that is more evident in the low sulfated CNC group.[15] In the three formulations evaluated, the 'soft' corona was characterized by the predominance of highly abundant PL proteins, namely, serum albumin (≈41% of total PL proteins), as reflected in the expanded spot at ≈67 kDa. Differences among the formulations were also observed in the profiles of the gel separated proteins, namely in the intensity of the bands at ≈55 kDa and ≈35 kDa, which can be attributed to fibrinogen gamma and apolipoprotein A–I, respectively.[16] In particular, the band at ≈35 kDa has higher intensity in M-CNC than in H-CNC and is barely seen in L-CNC. Next, PL–CNC complexes were extensively washed to remove loosely bound proteins and to analyze the proteins with high nanoparticle binding affinity. The band profile of the gel lanes shows differences in the 'hard' corona of the different CNC groups in terms of both protein composition and relative

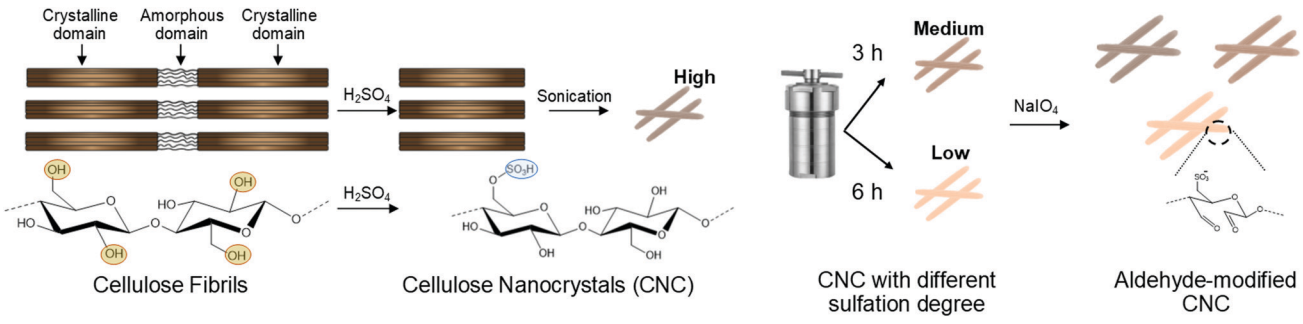

Fig. 1 Schematic representation of CNC production starting from microcrystalline cellulose and the typical sulfuric acid hydrolysis process that introduces sulfate groups on the surface. The CNC suspension (a high sulfate group content on the CNC surface) hydrothermally treated undergoes desulfation to obtain CNCs with different sulfation degrees (medium and low sulfate group content on the CNC surface), which are further aldehyde-modified by sodium periodate oxidation.

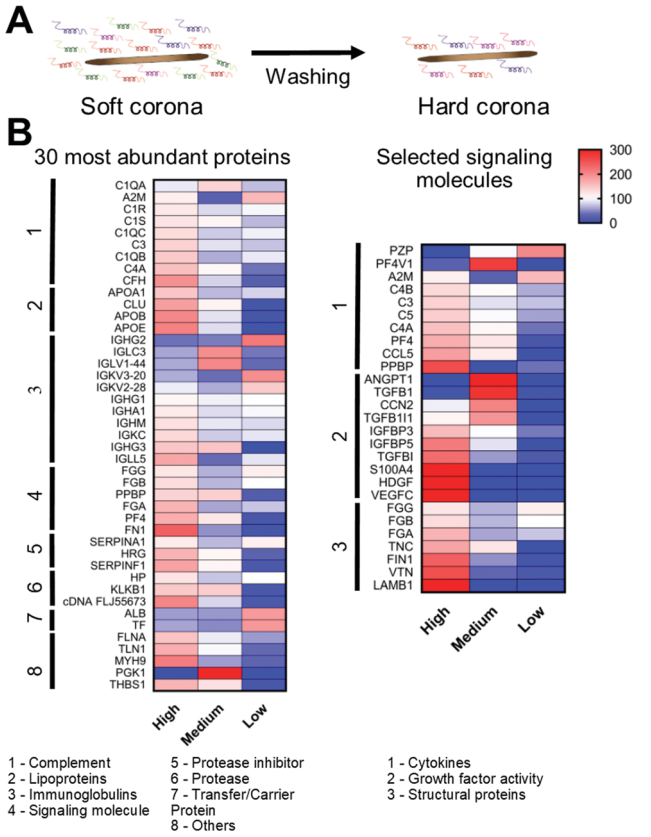

Fig. 2 Upon incubation with PL, (A) the initial CNC was decorated with a 'soft' corona that over time only retained the strong binding proteins. (B) The main components (30) found in the 'hard' corona and selected signaling molecules by their relative abundance and classified as Panther protein class. Red colour denotes higher counts and blue denotes lower than group average (set to 100, white).

quantity, particularly for the lower molecular weight bands like that at ≈15 kDa, which corresponds to the molecular weight of several GF monomers.[17] The protein compositions of the different 'hard' coronas were then evaluated in detail by proteomic analysis (Fig. S3B, ESI† and Fig. 2B). The total number of identified proteins was similar for the H-CNC (n = 702) and M-CNC (n = 638) groups, whereas it was lower for the L-CNC formulations (n = 491) (Fig. S3B, ESI†). The common and unique proteins in each formulation are represented as a Venn diagram. The homology between the coronas was ≈53%, ≈58% and ≈76% for H-CNC, M-CNC and L-CNC formulations, respectively. On the other hand, H-CNC has a higher fraction (≈18%) of unique proteins than M-CNC (≈10%) and L-CNC (≈13%). The identified proteins were then classified according to categories of biological response (Fig. S3B, ESI†). Although their distribution is in line with previous PL proteomic profiles,[18] differences can be observed not only in the total number of protein related processes but also in the relative weight of each category (Fig. S3B-i, ESI†). These differences are more evident when performing this analysis only on the unique proteins of each formulation. H-CNC shows a higher fraction of proteins related to a metabolic process (organic substance and cellular metabolic process) (Fig. S3B-ii, ESI†). Proteins related to biological regulation (biological process and molecular function) are more represented in M-CNC, whereas the L-CNC corona is richer in proteins related to processes of the immune system (leukocyte activation and immune effector process) (Fig. S3B-ii, ESI†).

Interestingly, the top 30 most abundant proteins accounted for over 80% of the total protein content in the coronas of the nanoparticles with the three different chemistries (Table S1, ESI†). The H-CNC corona has a high content of apolipoproteins ApoA1 and ApoE. The L-CNC corona was highly enriched with transfer/carrier proteins such as albumin (zinc, calcium and magnesium transporter) and serotransferrin (ferrous iron transporter), which may have a further role in stimulating cell growth and proliferation.[19] Collectively, detailed analysis of these results further suggests that electrostatic interactions are not the main driving mechanism in the development of CNC 'hard' coronas (Table S2 and Fig. S4, ESI†). Fig. 2B also highlights the adsorption pattern of different signaling molecules on an individual biomolecular corona, which shows the presence or complete absence of certain proteins depending on the sulfation degree of the CNC. For instance, hepatoma-derived GF and vascular endothelial GF-C (VEGF-C) were only found in the corona of H-CNC, whereas angiopoietin-1, which regulates angiogenesis,[20] and transforming growth factor beta-1 (TGF-β1) were only found in the corona of M-CNC. Moreover, H-CNC showed higher affinity for different structural proteins such as fibronectin and fibrinogen that have different peptide motifs in their structure involved in cell adhesion and regulation of GF signaling.[21] In addition, to explore the collective functions of the exclusive proteins identified in each formulation, we reconstructed network models describing the interactions among these proteins. Notably, it can be observed that, for example, in the M-CNC corona, there is an enrichment of proteins involved in hypoxia inducible factor-1 and VEGF signaling pathways (Fig. S6, ESI†). Overall, these results confirm that the 'hard' biomolecular corona adsorbed from PL on CNCs is surface chemistry dependent, and therefore, it might be able to entirely change the *in vitro* biological response of PL–CNC biomaterials. To test this hypothesis, thin films of different CNCs were spin-coated on cell culture glass coverslips (Fig. S8, ESI†), incubated with PL solutions and then washed to remove the 'soft' biomolecular corona. Human adipose-derived stem cells (hASCs) were seeded on these substrates and cultured *in vitro* to evaluate their biological behavior. Overall, the cells proliferated faster on M-CNC and L-CNC than on H-CNC, although cell numbers tended to level-off by day 28 (Fig. S9A, ESI†). Cell morphology and cell spreading area were also evidently different among the groups (Fig. 3A and Fig. S9B, ESI†). Histological staining was used as a first screening technique to evaluate the effect of the different CNCs on the potential cell commitment to three common mesenchymal lineages (chondrogenic, osteogenic and adipogenic). While all groups stained negative for Oil red O and Alizarin red (Fig. S10, ESI†), hASCs seeded onto M-CNC stained positive for Alcian Blue, indicating an increased content of sulfated GAGs in the newly cell deposited ECM, as shown in Fig. 3B and Fig. S10 (ESI†). Considering the positive staining for this marker, which

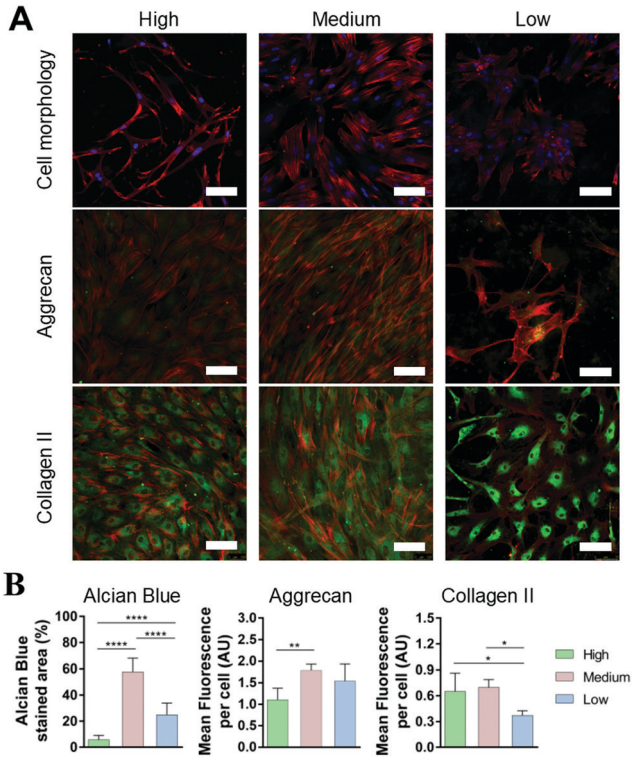

Fig. 3 (A) *In vitro* evaluation of hASC behaviour. Fluorescence microscopy images showing cell morphology at day 7, and aggrecan and collagen type II expression at day 28. (B) Quantification of mean fluorescence intensity of Alcian blue staining by coverage staining area, and aggrecan and collagen II by cell nuclei. Staining actin (red), nuclei (blue), aggrecan and collagen type II (green). Scale bar: 100 μm.

is usually related with the chondrogenic commitment of stem cells, we then evaluated the expression of other markers related to this lineage, namely, aggrecan and collagen type II, by immunochemistry (Fig. 3A and B). Consistent with the histological staining result, the M-CNC group also revealed an increased expression of these cartilaginous markers. Although this cell behavior might result from a synergistic effect of several signaling biomolecules, it is interesting to notice that, *e.g.*, TGF-β1 and CCN family member 2, two GFs known to stimulate cell adhesion and proliferation as well as to induce chondrogenic differentiation of stem cells, were upregulated in the M-CNC group (Fig. 2).[22] Altogether, these results demonstrate that the different CNC surface chemistries led to different corona compositions of PL proteins. The sequestering and presentation of tailored protein coronas to cell receptors can activate different cell signaling pathways and guide cell fate decisions. The novel concept proposed here thus has the potential to enable the development of a portfolio of PL–CNC engineered biomaterials with tissue specific bioactivity that could find broad applications as artificial ECMs in organotypic TE strategies.

The research has received funding from PTDC/NAN-MAT/30595/2017, ERC Grant No. 772817; FCT/MCTES for PD/59/2013 - PD/BD/113807/2015, for ITI Research grant 1306_2018, ROTEIRO/0028/2013, and LISBOA-01-0145-FEDER-022125.

Conflicts of interest

There are no conflicts to declare.

References

1 D. Klemm, E. D. Cranston, D. Fischer, M. Gama, S. A. Kedzior, D. Kralisch, F. Kramer, T. Kondo, T. Lindström, S. Nietzsche, K. Petzold-Welcke and F. Rauchfuß, *Mater. Today*, 2018, **21**, 720.
2 B. B. Mendes, M. Gómez-Florit, R. A. Pires, R. M. A. Domingues, R. L. Reis and M. E. Gomes, *Nanoscale*, 2018, **10**, 17388.
3 B. B. Mendes, M. Gómez-Florit, P. S. Babo, R. M. Domingues, R. L. Reis and M. E. Gomes, *Adv. Drug Delivery Rev.*, 2018, **129**, 376.
4 (*a*) P. C. Ke, S. Lin, W. J. Parak, T. P. Davis and F. Caruso, *ACS Nano*, 2017, **11**, 11773; (*b*) M. P. Monopoli, C. Åberg, A. Salvati and K. A. Dawson, *Nat. Nanotechnol.*, 2012, **7**, 779.
5 C. Corbo, R. Molinaro, A. Parodi, N. E. Toledano Furman, F. Salvatore and E. Tasciotti, *Nanomedicine*, 2015, **11**, 81.
6 M. Mahmoudi, I. Lynch, M. R. Ejtehadi, M. P. Monopoli, F. B. Bombelli and S. Laurent, *Chem. Rev.*, 2011, **111**, 5610.
7 (*a*) S. Schöttler, K. Landfester and V. Mailänder, *Angew. Chem., Int. Ed.*, 2016, **55**, 8806; (*b*) J. O'Brien and K. J. Shea, *Acc. Chem. Res.*, 2016, **49**, 1200.
8 (*a*) D. Bondeson, A. Mathew and K. Oksman, *Cellulose*, 2006, **13**, 171; (*b*) M. S. Reid, M. Villalobos and E. D. Cranston, *Langmuir*, 2017, **33**, 1583.
9 D. Xu and J. D. Esko, *Annu. Rev. Biochem.*, 2014, **83**, 129.
10 (*a*) J. E. Scott, *Pathol. Biol.*, 2001, **49**, 284; (*b*) T. Miller, M. C. Goude, T. C. McDevitt and J. S. Temenoff, *Acta Biomater.*, 2014, **10**, 1705; (*c*) N. S. Gandhi and R. L. Mancera, *Chem. Biol. Drug Des.*, 2008, **72**, 455.
11 S. S. Lee, T. Fyrner, F. Chen, Z. Álvarez, E. Sleep, D. S. Chun, J. A. Weiner, R. W. Cook, R. D. Freshman, M. S. Schallmo, K. M. Katchko, A. D. Schneider, J. T. Smith, C. Yun, G. Singh, S. Z. Hashmi, M. T. McClendon, Z. Yu, S. R. Stock, W. K. Hsu, E. L. Hsu and S. I. Stupp, *Nat. Nanotechnol.*, 2017, **12**, 821.
12 L. Lewis, M. Derakhshandeh, S. G. Hatzikiriakos, W. Y. Hamad and M. J. MacLachlan, *Biomacromolecules*, 2016, **17**, 2747.
13 (*a*) D. Peschel, K. Zhang, N. Aggarwal, E. Brendler, S. Fischer and T. Groth, *Acta Biomater.*, 2010, **6**, 2116; (*b*) D. Peschel, K. Zhang, S. Fischer and T. Groth, *Acta Biomater.*, 2012, **8**, 183.
14 (*a*) I. Kalashnikova, H. Bizot, B. Cathala and I. Capron, *Biomacromolecules*, 2012, **13**, 267; (*b*) C. Bruel, J. R. Tavares, P. J. Carreau and M.-C. Heuzey, *Carbohydr. Polym.*, 2019, **205**, 184.
15 A. Gessner, A. Lieske, B. R. Paulke and R. H. Müller, *Eur. J. Pharm. Biopharm.*, 2002, **54**, 165.
16 S. Kinzebach, L. Dietz, H. Klüter, H.-J. Thierse and K. Bieback, *BMC Cell Biol.*, 2013, **14**, 48.
17 P.-J. Yu, G. Ferrari, A. C. Galloway, P. Mignatti and G. Pintucci, *J. Cell. Biochem.*, 2007, **100**, 1100.
18 S. Viau, A. Lagrange, L. Chabrand, J. Lorant, M. Charrier, K. Rouger, I. Alvarez, S. Eap and B. Delorme, *Cytotherapy*, 2019, **21**, 738.
19 (*a*) A. W. M. Lee, P. S. Oates and D. Trinder, *Hepatology*, 2003, **38**, 967; (*b*) G. L. Francis, *Cytotechnology*, 2010, **62**, 1.
20 H. G. Augustin, G. Young Koh, G. Thurston and K. Alitalo, *Nat. Rev. Mol. Cell Biol.*, 2009, **10**, 165.
21 (*a*) V. Llopis-Hernández, M. Cantini, C. González-García, Z. A. Cheng, J. Yang, P. M. Tsimbouri, A. J. García, M. J. Dalby and M. Salmerón-Sánchez, *Sci. Adv.*, 2016, **2**, e1600188; (*b*) M. M. Martino, P. S. Briquez, A. Ranga, M. P. Lutolf and J. A. Hubbell, *Proc. Natl. Acad. Sci. U. S. A.*, 2013, **110**, 4563.
22 I. B. Robertson and D. B. Rifkin, *Cold Spring Harbor Perspect. Biol.*, 2016, **8**, a021907.